CHEMICAL ENGINEERING TRANSACTIONS
VOL. 101, 2023
A publication of AIDIC
The Italian Association of Chemical Engineering
Online at www.cetjournal.it
Guest Editors: Paolo Ciambelli, Luca Di Palma
Copyright © 2023, AIDIC Servizi S.r.l.
ISBN 979-12-81206-00-7; **ISSN** 2283-9216
DOI: 10.3303/CET23101022

Synthesis and CO_2 Adsorption Capacity of Biomass Waste Functionalized by Nanoparticles

Domenico Rosa, Valentina Segneri*, Luca Di Palma, Giorgio Vilardi

Department of Chemical Engineering Materials Environment & UdR INSTM, Sapienza-Università di Roma, Via Eudossiana 18, 00184 Roma, Italy
valentina.segneri@uniroma1.it

Two composite materials were synthesized based on sodium alginate and biochar derived from licorice processing waste functionalized with silicon dioxide nanoparticles (SiO_2) and iron oxide (Fe_2O_3), respectively, enabling the valorization of industrial waste. The adsorptive capacities of the two materials (Alg-SiO_2 and BC_L-Fe_2O_3) toward CO_2 in the gaseous stream with nitrogen were evaluated by acid titration of carbonates present in a trap for CO_2 consisting of a KOH solution placed downstream of the adsorption column. The aim of the present work is to evaluate the CO_2 adsorption capacity of material functionalized by nanoparticles. Adams–Bohart, Thomas models, and % removal efficiency curves for the adsorption were examined to investigate the dynamic behavior of the column. From the tests performed in CO_2 and N_2 flow, the BC_L-Fe_2O_3 material was demonstrated to have an adsorbent higher capacity than Alg-SiO_2, respectively CO_2 adsorbed 25 and 6 mg/g.

1. Introduction

Global warming effects from excessive greenhouse gas emissions, such as CO2, are now becoming a serious environmental problem (Trinca et al., 2022).
Many strategies have been developed to solve this, with the advancement of nanoscience and nanotechnology, direct CO_2 becomes an effective strategy to capture CO2 and transform it directly into compounds valuable chemicals in delicate environments. (Lu et al., 2021).
Among the many sorbents, char made from the carbonization of biomass waste has been found to have exceptional CO_2 adsorption capabilities. Carbon-based adsorbents, due to their large surface area, ability to pore size modification and ease of turnover, low cost of preparation, and low impact are considered to be one of the best materials for CO_2 sequestration (Goel et al., 2021).
Commonly, converting biomass into porous carbons for CO_2 capture includes carbonization, activation through exposure to high temperature and CO_2 and steam environments (physical activation) or using potassium hydroxide KOH (chemical activation), and surface modification by addition of additives like metal oxides, that can potentially improve the surface chemistry and adsorption chemistry by improving the interaction between the adsorbent surface and the CO_2 molecule (Akeeb et al., 2022).
In this work, two composite materials functionalized with nanoparticles have been synthesized: the first based on sodium alginate functionalized with silicon dioxide nanoparticles (SiO_2), while the second formed by iron oxide nanoparticles supported on a lignocellulosic matrix (biochar derived from licorice), thus allowing the valorization of an industrial waste.
Silica-based nanoparticles have attracted considerable interest from researchers due to their high surface area, large pore volume, narrow pore size distribution, and excellent regeneration stability of silica. On the other hand, adsorbents based on iron oxides are efficient reversible sorbents for CO_2 capture.
The technique for CO_2 adsorption made from biomass might be proven to be one of the most affordable and environmentally beneficial ways to combat climate change.

Paper Received: 18 December 2022; Revised: 11 April 2023; Accepted: 13 May 2023
Please cite this article as: Rosa D., Segneri V., Di Palma L., Vilardi G., 2023, Synthesis and CO_2 adsorption capacity of biomass waste functionalized by nanoparticles , Chemical Engineering Transactions, 101, 127-132 DOI:10.3303/CET23101022

2. Materials and methods

2.1 Chemicals

In this work, the following reagents are employed: silicon dioxide (Carlo Erba), hexahydrated ferric chloride ($FeCl_3$*$6H_2O$, Honeywell), sodium alginate (Special Ingredients), sodium hydroxide (NaOH, Honeywell), potassium hydroxide (KOH, Honeywell), phenolphthalein (Carlo Erba), sulfuric acid (H_2SO_4 98 %, Honeywell), nitric acid (HNO_3 64 % Honeywell) acetic acid (CH_3COOH glacial, Carlo Erba), hydrochloric acid (HCl 37 %, Honeywell), licorice roots waste (Amarelli). All the chemicals were used without any further purification. Demineralized water was used as a solvent for both solutions.

2.2 Composite materials synthesis

Synthesis of SiO_2 nanoparticles supported on alginate (Alg-SiO_2) was performed by preparing a 1 wt% aqueous solution of alginate by dissolving sodium alginate (1.2 g) in a 1 wt% aqueous solution of acetic acid (1.2 ml in 120 ml of water) under constant magnetic stirring until achieving a homogeneous solution (400 rpm for 2 h). The alginate solution was then immersed in the suspension of SiO_2 nanoparticles (6.1 g in 1000 ml) and placed in an ultrasonic bath for 20 minutes. Then the mixture was maintained at 60 °C for 4 h under constant stirring at 400 rpm and subsequently placed in an ice water bath for 1 h. The sample was centrifuged at 10000 rpm for 10 min, the solid was separated from the liquid and placed in an oven at 60 °C overnight. The sample Alg-SiO_2 was obtained (Figure 1).
Synthesis of Fe_2O_3 nanoparticles supported on BC_L (BC_L-Fe_2O_3) was performed in two steps. First, BC_L was prepared from licorice processing waste by washing the licorice roots with plenty of water to remove soil and other impurities. The roots were then placed in an oven at 60 °C overnight. Then they were ground and sieved through a 1 mm sieve and placed in an autoclave and pressed to make the environment as anoxic as possible. The sample was placed in a muffle furnace at 700 °C for 2 h thus obtaining BC_L.
10 g of BC_L were then functionalized by holding it at 60 °C for 4 h under constant magnetic stirring at 400 rpm in 200 ml of an acid solution made of 10 ml HNO_3 (64 %) and 30 ml H_2SO_4 (98 %) to form carboxylic groups on the BC surface. After the solid was washed with demineralized water until neutral pH and dried in an oven at 60 °C overnight. Then 10 g of functionalized BC_L were dispersed in 200 ml of an aqueous solution containing 0.6 mol of $FeCl_3$ and magnetically stirred for 2h at 60 °C. After that, 100 ml of NaOH 2 M solution was added to the mixture dropwise and magnetically stirred for 2h at 60 °C. After the solid was filtered and washed with demineralized water until neutral pH and dried in an oven at 60 °C overnight. Finally, the solid was calcined in muffle at 600 °C for 1 h obtaining BC_L-Fe_2O_3 sample (Figure 1).

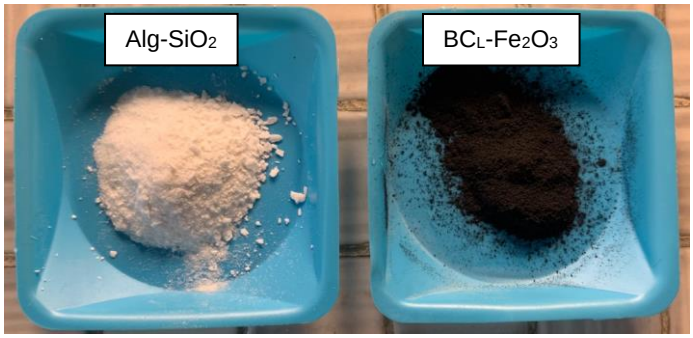

Figure 1: Synthesized materials: at left SiO_2-based sample supported on alginate (Alg-SiO_2) and at right Fe_2O_3-based sample supported on licorice biochar (BC_L-Fe_2O_3).

2.3 Experimental setup

The experimental set-up consisted of two gas cylinders of CO_2 and N_2. The flow rate used for the tests was 40 ml/min for CO_2 and 60 ml/min for N_2 and was controlled by flowmeters placed before a Y-valve that would allow the mixing of the two gases before reaching the adsorbent column, which consisted of a tubular polyethylene reactor of volume 10 ml and diameter 0.5 cm inside of which the adsorbent material was placed until full; 12.02 g of Alg-SiO_2 and 3.98 g of BC_L-Fe_2O_3 were employes, this different amount is due to the huge difference in density of the two solids. Paper filters were placed to support the adsorbent material both at the head and tail, and the column was placed horizontally to the work surface. The gas stream leaving the column was directed into a cylinder containing a 1 L 2M KOH solution to convert CO_2 to carbonate ion according to the following equation (Eq. 1):

$$CO_2 + KOH = CO_3^{2-} + H^+ + K^+ \quad (1)$$

The experimental set-up is illustrated below (Figure 2):

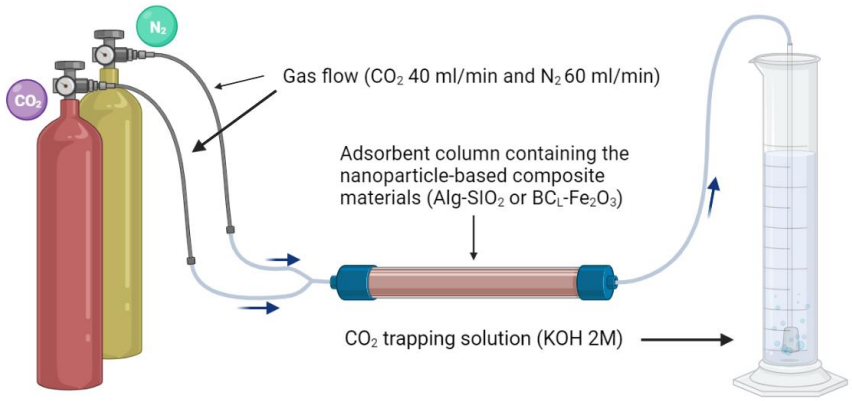

Figure 2: Experimental set-up used to carry out adsorption CO_2 employing based nanoparticles composite materials (Alg-SiO_2 and BC_L-Fe_2O_3).

2.4 Evaluation of CO_2 adsorption capacity

As soon as the gas flowed, at room temperature, 10 mL samples each were taken at different times (0-180 min) of CO_2 trapping solution (no additional solution was added to compensate for the decrease in volume due to withdrawals but was considered in the calculation of carbonate moles) employing both columns containing the two different materials and without any column as a checking test. All samples taken were titrated using a known titer solution of HCl and drops of saturated phenolphthalein solution with a characteristic fuchsia color. Phenolphthalein is the ideal indicator for titration of carbonates because the color change (from fuchsia to transparent) occurs at pH 8.3, which corresponds to the pH below which the carbonate ions protons into the bicarbonate ions. Knowing the moles of acid needed for titration, it was possible to derive the moles of carbonate. Having calculated the concentration of carbonate ions in the samples, it was possible to derive the adsorptive capacity of the materials toward CO_2 (defined as mg of CO_2 adsorbed per g of material) by the difference between checking and adsorbent column tests and normalizing by the weight of the solid employed. As further verification, the samples were acidified with drops of HCl to lower the pH to about 6 and analyzed for inorganic carbon by Shimadzu TOC-L analyzer.

2.5 Breakthrough curve modeling

An exceptional overview of the column adsorption process primarily requires prediction of the break-through curve for effluent. Several simplistic models of packed bed dynamics to describe and analyze lab-scale studies are mainly used in industrial applications. In order to predict column dynamics, the Adams–Bohart, Thomas, Yoon and Wang models were used to fit adsorption breakthrough data (Subbaiah et al., 2011). These fixed bed models are popular because their model equations can be linearized, allowing their unknown parameters to be estimated by linear regression analysis (Chu, 2020).

In this work, to evaluate the performance, Adams–Bohart model was used. To analyze the Adams–Bohart model parameter the value of rate constant decreases with increase of influent concentration.

The century-old Bohart-Adams model is arguably the best known one which also serves as the foundation of the bed depth-service time equation. Bohart and Adams (S Bohart and Adams, 2023) described the relationship between C_t/C_0 and t in a continuous system, which is used for describing the initial part of the breakthrough curve. The expression is as follows:

$$\frac{C_0}{C_t} = \begin{cases} \dfrac{\exp\left(k_{AB}C_0\left(t-\frac{\varepsilon Z}{U_0}\right)\right)}{\exp(k_{AB}N_0(Z/U_0)) + \exp\left(k_{AB}C_0\left(t-\frac{\varepsilon Z}{U_0}\right)\right) - 1}, & t > \dfrac{\varepsilon Z}{U_0} \\ 0, & 0 < t < \dfrac{\varepsilon Z}{U_0} \end{cases} \quad (2)$$

where C_0 and C_t are the influent and effluent concentration (g/L), k_{AB} is the Bohart Adams kinetic constant (L/gmin), N_0 is the adsorption capacity of the adsorbent per unit volume of the bed (g/L), ε is the bed voidage, Z is the bed depth of the fix-bed column (cm) and U_0 is the superficial velocity (cm/min) defined as the ratio of the volumetric flow rate Q (cm^3/min) to the cross-sectional area of the bed A (cm^2), k_{AB} and N_0 can be calculated from the linear plot of $ln(C_t/C_0)$ against time.

Their model assumes that the adsorbate is adsorbed irreversibly and at a local rate of removal that is proportional to both the residual capacity of the adsorbent and the gas phase concentration of the adsorbate.

A key feature of the 100-year-old model of Bohart and Adams (Chu, 2020) is that it predicts a linear relationship between bed depth and the time taken for breakthrough to occur. This linear relationship simplifies the tasks of adsorber design and analysis and provides a simple approach to running pilot tests.

Since the exponential term $exp\left(\frac{k_{AB}N_0Z}{U_0}\right)$ is expected to be much larger than unity and t is usually much greater than $\varepsilon Z/U_0$.

$$ln\left(\frac{C_0}{C_t}-1\right)=k_{AB}N_0\left(\frac{Z}{U_0}\right)-k_{AB}C_0(t) \quad (3)$$

3. Results and discussions

3.1 Adsorption performances

Figure 3 shows the capture kinetic curve for each of the composite materials.

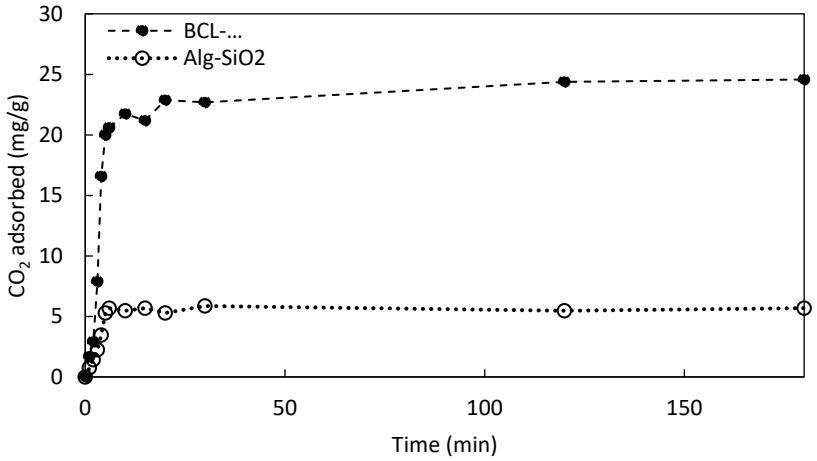

Figure 3: CO_2 adsorption kinetics of two different materials BC_L-Fe_2O_3 and Alg-SiO_2 using respectively 3.98 and 12.02 g, gas flow 40 ml/min for CO_2 and 60 ml/min for N_2 at room temperature.

From the data shown in Figure 3 the significant difference in the adsorption capacity of the two materials was evident, in fact Alg-SiO_2 showed an adsorptive capacity of 6 mg/g while BC_L-Fe_2O_3 of 25 mg/g under the conditions employed (room temperature and flow of CO_2 40 ml/min and N_2 60 ml/min) in agreement with other authors (KIRBIYIK, 2019; Rafigh and Heydarinasab, 2017). This result could be justified by the different properties of the materials, primarily to the surface area and porosity but also other factors such as interactions with functional groups on the surface could play an important role in CO_2 adsorption. It is known that there are nitrogen groups present on the surface of biochars that are weakly basic and polar (combination of physical and chemical adsorption) and could increase the adsorption capacity of CO_2. (Zhang et al., 2013). Another important difference is due to the nature of iron oxide, which has weakly basic properties which is advantageous in terms of capturing CO_2 that is acidic, whereas sicile is known to be an oxide with acidic characteristics (Schott et al., 2017).

3.2 Breakthrough curve modeling

The following figures show the comparison between the experimental values of the C/C_0 ratio, and the breakthrough curve determined using the Adams Bohart model.

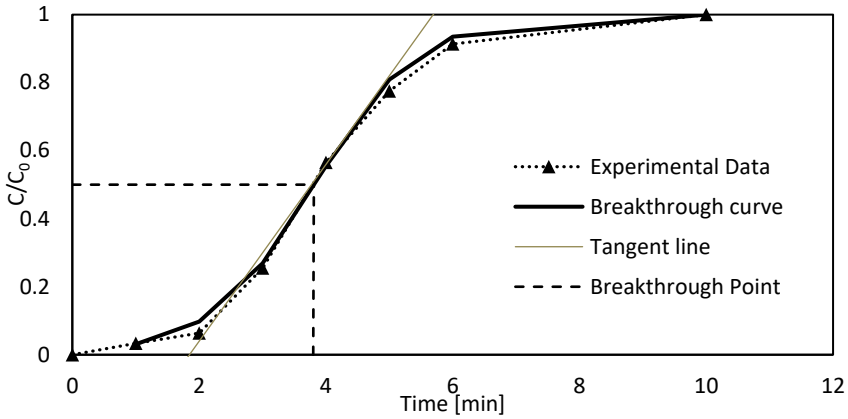

Figure 4: Breakthrough curve of Alg-SiO_2 using Adams - Bohart Model, where K_{AB} *= 0.081 L/(gmin) and* N_0 *= 562 g/L (with* $R^2 = 99.81\%$*).*

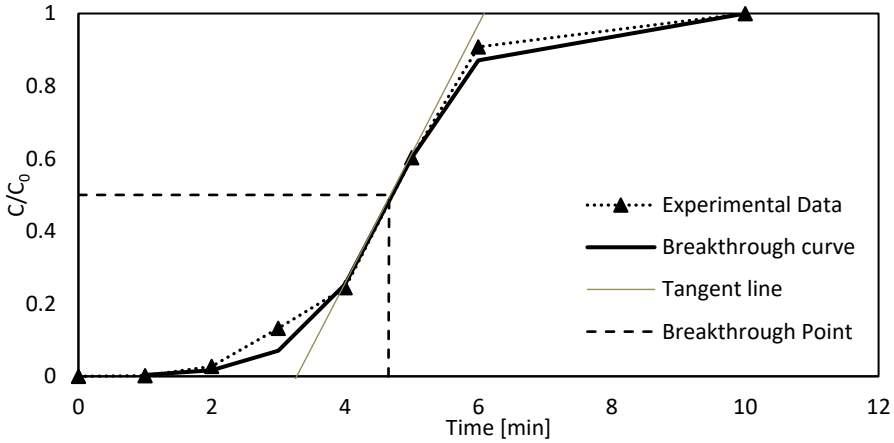

Figure 5: Breakthrough curve of BC_L*-*Fe_2O_3 *using Adams - Bohart Model, where* K_{AB} *= 0.23 L/gmin and* N_0 *= 299 g/L (with* $R^2 = 99.63\%$*).*

The data points in the initial part of the failure curve indicate that failure of the tested materials occurred almost immediately. A large increase in the dimensionless effluent concentration to approximately 70% was followed by a relatively slow approach to saturation, a characteristic of tailing that has been attributed to a variety of factors, including non-specific adsorption or flow non-uniformity. Accounting for these possible stalking causes mechanistically requires the use of complex models.
The following Table shows the values of the parameters determined using the Adams - Bohart model. As can be seen, the iron oxide particles supported on a lignocellulosic matrix have a higher kinetic constant than Alg-SiO_2 ones, managing to adsorb CO_2 faster.

Table 1: Adams Bohart Model Parameter

	Adams - Bohart		
$Alg - SiO_2$	N_0 [g/l]	K_{AB} [l/gmin]	R^2
	562	0.081	99.81%
$BC_L - Fe_2O_3$	N_0 [g/l]	K_{AB} [l/gmin]	R^2
	299	0.23	99.63%

4. Conclusions

This study presents a novel method to capture CO_2 from two nanoparticle-functionalized matrix-based composite materials. The experimental phase was carried out using 40 ml/min for CO_2 and 60 ml/min for N_2 conveyed in an adsorbent column, consisting of a tubular polyethylene reactor with a volume of 10 ml.
From tests performed in CO_2 and N_2 flow (40 and 60 ml/min), it was demonstrated that the BC_L-Fe_2O_3 material has a higher adsorbing capacity than Alg-SiO_2, CO_2 adsorbed 25 and 6 m/g respectively due to the different nature of the materials and also to the different synthesis strategy. From the analysis of the results and mediated modeling of the Adams Bohart model, the BC_L-Fe_2O_3 material has been shown to have a higher kinetic constant than Alg-SiO_2, showing good CO_2 adsorption capacity.
These results confirm what was reported in previous studies concerning iron oxide-based adsorbents, which are prospective and efficient adsorbents for CO_2 capture.

Acknowledgement

The authors acknowledge Sapienza and EU for the project funded under the National Recovery and Resilience Plan (NRRP), of Italian Ministry of Research funded by the European Union – NextGenerationEU: Partnerships extended to Universities, Research Centres, Companies for Funding Basic Research Projects
The authors also recognize the financial support by “Sapienza” University of Rome for grant no. RM120172A298917B.

References

Akeeb, O., Wang, L., Xie, W., Davis, R., Alkasrawi, M., Toan, S., 2022. Post-combustion CO2 capture via a variety of temperature ranges and material adsorption process: A review. J Environ Manage 313, 115026. https://doi.org/10.1016/j.jenvman.2022.115026

Chu, K.H., 2020. Breakthrough curve analysis by simplistic models of fixed bed adsorption: In defense of the century-old Bohart-Adams model. Chemical Engineering Journal 380. https://doi.org/10.1016/j.cej.2019.122513

Goel, C., Mohan, S., Dinesha, P., 2021. CO2 capture by adsorption on biomass-derived activated char: A review. Science of the Total Environment 798, 149296. https://doi.org/10.1016/j.scitotenv.2021.149296

KIRBIYIK, Ç., 2019. Modification of biomass-derived activated carbon with magnetic-Fe2O3nanoparticles for CO2and CH4adsorption. Turk J Chem 43, 687–704. https://doi.org/10.3906/kim-1810-32

Lu, C., Shi, X., Liu, Y., Xiao, H., Li, J., Chen, X., 2021. Nanomaterials for adsorption and conversion of CO2 under gentle conditions. Materials Today 50, 385–399. https://doi.org/10.1016/j.mattod.2021.03.016

Rafigh, S.M., Heydarinasab, A., 2017. Mesoporous Chitosan-SiO2 Nanoparticles: Synthesis, Characterization, and CO2 Adsorption Capacity. ACS Sustain Chem Eng 5, 10379–10386. https://doi.org/10.1021/acssuschemeng.7b02388

S Bohart, B.G., Adams, E.Q., 2023. SOME ASPECTS OF THE BEHAVIOR OF CHARCOAL WITH RESPECT TO CHLORINE.1. UTC.

Schott, J.A., Wu, Z., Dai, S., Li, M., Huang, K., Schott, J.A., 2017. Effect of metal oxides modification on CO2 adsorption performance over mesoporous carbon. Microporous and Mesoporous Materials 249, 34–41. https://doi.org/10.1016/j.micromeso.2017.04.033

Subbaiah, M.V., Yuvaraja, G., Vijaya, Y., Krishnaiah, A., 2011. Equilibrium, kinetic and thermodynamic studies on biosorption of Pb(II) and Cd(II) from aqueous solution by fungus (Trametes versicolor) biomass. J Taiwan Inst Chem Eng 42, 965–971. https://doi.org/10.1016/j.jtice.2011.04.007

Trinca, A., Segneri, V., Mpouras, T., Libardi, N., Vilardi, G., 2022. Recovery of Solid Waste in Industrial and Environmental Processes. Energies (Basel). https://doi.org/10.3390/en15197418

Zhang, C., Song, W., Sun, G., Xie, L., Wang, J., Li, K., Sun, C., Liu, H., Snape, C.E., Drage, T., 2013. CO2 capture with activated carbon grafted by nitrogenous functional groups, in: Energy and Fuels. pp. 4818–4823. https://doi.org/10.1021/ef400499k